Spatially Heterogeneous Water Properties at Disordered Surfaces Decrease the Hydrophobicity of Nonpolar Self-Assembled Monolayers

Bradley C. Dallin and Reid C. Van Lehn*

Department of Chemical and Biological Engineering, University of Wisconsin – Madison, 1415 Engineering Drive, Madison, WI, 53706 USA

*send correspondence to: vanlehn@wisc.edu

Abstract

Understanding the relationship between hydrophobicity and the properties of functionalized surfaces is vital to the design of materials that interact in aqueous environments. In this Letter, we use atomistic molecular dynamics simulations to investigate the effects of surface order on the hydrophobicity of self-assembled monolayers (SAMs) containing nonpolar ligands. We find that the interfacial hydrophobicity is highly correlated with SAM order and, strikingly, poorly correlated with the solvent-accessible surface area, which typically has been related to interfacial hydrophobicity. Analysis of spatial variations in both SAM and water properties reveals that the SAM-water interface is pinned near regions of disordered SAM surfaces with increased free volume, decreasing the overall interfacial hydrophobicity. Spatial variations in ligand end group positions at disordered SAM surfaces thus translate to spatial variations in hydrophobicity, yielding heterogeneous surface properties. These findings provide new insights into how surface order can alter the hydrophobicity of chemically uniform surfaces.

TOC Graphic

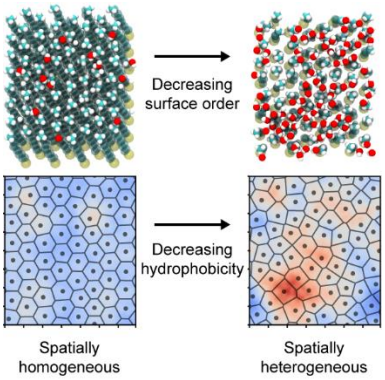

In aqueous environments, nonpolar solutes are driven to associate by water-mediated hydrophobic interactions that are important for the stability of colloids,[1-2] the assembly of biological macromolecules,[3-5] and the adsorption of peptides and proteins to functionalized surfaces.[6-9] Hydrophobic interactions emerge from the inability of water molecules to form hydrogen bonds with nonpolar materials, leading to the thermodynamically unfavorable disruption of interfacial water structure that is minimized by bringing nonpolar surface area into contact.[10] The interplay of solute-water and water-water interactions thus determines the hydrophobicity of an interface. The hydrophobicity of uniformly nonpolar solutes scales with surface area for a large solute with a radius greater than ~1 nm; the hydrophobicity of a small solute with a radius less than ~1 nm instead scales with volume.[10] The hydrophobicity of more complex interfaces is less easily characterized; for example, interfacial hydrophobicity has been shown to be depend on the number and spatial location of both polar and nonpolar amino-acid residues in proteins[11-13] and in peptides,[14-16] and both the composition and patterning of hydrophilic groups on silica and self-assembled monolayer (SAM) surfaces.[17-18] These studies show that interfacial hydrophobicity depends on collective interactions at chemically heterogeneous interfaces in which polar, charged, and nonpolar moieties are in close proximity and cannot be predicted from the properties of individual interfacial groups as is sometimes assumed.[19-21]

Interfacial hydrophobicity also depends on physical properties, such as the local curvature.[22] We recently demonstrated that the hydrophobicity of planar, uniformly nonpolar SAMs composed of alkanethiol ligands depends on ligand length and saturation.[23-24] Using molecular dynamics (MD) simulations, we found that short ligands exhibit pronounced fluctuations and are highly disordered whereas longer ligands exhibit minimal fluctuations and are quasi-crystalline. Interfacial water molecules are more structured near SAMs with short ligands compared to water molecules near SAMs with longer ligands, resembling the same difference in water structure observed for small and large uniformly nonpolar solutes.[10] Accordingly, simulations showed that hydrophobic interactions between SAMs strengthened with increasing ligand length in agreement with experimental measurements.[23-24] This finding raises questions regarding the distinct effects that SAM fluctuations or order could have on hydrophobicity, as these effects were not distinguished in our prior study. For example, separate studies have identified a potential role of fluctuations on the hydrophobicity of chemically heterogeneous SAMs[17] and the effect of order on interfacial water structure for model surfaces.[25] Distinguishing these effects could provide further insight into the hydrophobicity of soft materials, such as lipid bilayers, proteins, or functionalized nanomaterials.

In this study, we use MD simulations to investigate the effect of SAM order on interfacial hydrophobicity by decoupling SAM order from ligand fluctuations. We hypothesize that if the timescale for ligand fluctuations is slower than the relaxation time of interfacial water molecules, then the order of SAM configurations sampled due to fluctuations should dictate interfacial hydrophobicity. We first confirm that the timescale for SAM reorganization due to ligand fluctuations is much greater than that of interfacial water dynamics, then use enhanced-sampling techniques to identify a linear correlation between interfacial hydrophobicity and order for SAMs in which fluctuations are inhibited. Analysis of these configurations shows that disordered SAM configurations have significant free volume that permits the penetration of water molecules into the SAM to behave like interfacial hydroxyl groups. This behavior leads to spatial variations in hydrophobicity that resemble the spatial variations at chemically heterogeneous interfaces. These findings provide new insight into how the molecular-level order of chemically homogeneous surfaces can impact hydrophobicity.

We modeled single-component SAMs composed of alkanethiol ligands based on our prior work.[24] Figure 1 shows the structure of a short, butanethiol ligand that forms a disordered, liquid-like SAM with large fluctuations and the structure of a long, dodecanethiol ligand that forms an ordered, quasi-crystalline SAM with minimal fluctuations.[23, 26] SAMs were modeled by placing alkanethiol ligands in positions corresponding to the hexagonal Au(111) lattice with sulfur atoms restrained by harmonic potentials to retain the ligand arrangement.[27] The gold substrate was not modeled because it was not shown to impact hydrophobicity in our prior work.[24] SAMs were solvated by a 5 nm water layer and a 3.5 nm vacuum layer was then added to prevent interactions between ligand sulfur atoms and water. The vacuum layer further

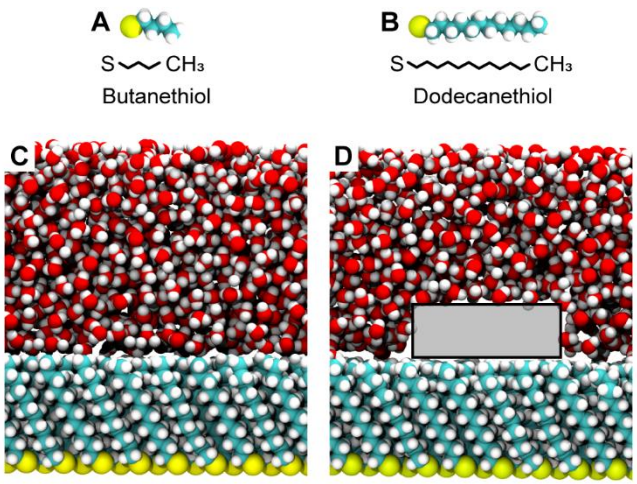

Figure 1. Simulation and chemical representations of the butanethiol (**A**) and dodecanethiol (**B**) ligands, and representative simulation snapshots for a dodecanethiol SAM before (**C**) and after (**D**) using INDUS to dewet an interfacial cavity (indicated by the gray box in **D**).

served as a volume buffer during *NVT* simulations.[28] Details on the simulation methods and force field parameters are provided in SI Section S1.[24]

We quantified SAM hydrophobicity by measuring the hydration free energy, or excess chemical potential, μ_v, at the SAM-water interface. μ_v is the free energy change for dewetting a cavity of a specific volume (denoted by v) which is related to the probability that zero water molecules occupy the cavity, $p_v(0)$, by Equation 1.

$$\mu_v = -k_B T \ln p_v(0) \tag{1}$$

μ_v depends on the cavity location, shape, and volume. The value of μ_v for a cavity placed near an interface can be used as a molecular indicator of interfacial hydrophobicity: a larger value of μ_v indicates a lower likelihood of dewetting and thus a more hydrophilic interface.[28] For small spherical cavities (with radii less than 0.5 nm), μ_v can be determined by calculating $p_v(0)$ in unbiased simulations.[29] However, $p_v(0)$ is extremely small for larger cavities. To overcome this challenge, we employed indirect umbrella sampling (INDUS), an enhanced-sampling technique that calculates μ_v by applying a biasing potential to expel water molecules from the cavity.[30] INDUS simulation details are presented in SI Section S2.[28, 30] We performed INDUS simulations to measure the hydration free energy for a 2.0 x 2.0 x 0.8 nm^3 cavity near the SAM surface, which we define as μ_A. The SAM surface is defined as the average z-position of the end group carbon atoms (*i.e.*, the carbon atoms at the SAM-water interface) and the cavity is positioned relative to the SAM surface based on the water density as described in SI Section S2. μ_A was determined for six alkanethiol SAMs to compare to prior work in which we measured hydrophobic interactions between apposed SAMs.[24] Figure 2 shows that μ_A decreases with increasing ligand length. We also find that μ_A is significantly larger for a SAM containing unsaturated ligands (red square in Figure 2) compared to a SAM with saturated ligands of the same length. These results match trends obtained from prior simulations of hydrophobic interactions and from experimental atomic force microscopy measurements (Figure S7),[24] indicating that μ_A can be used to compare differences in SAM hydrophobicity that should correlate with hydrophobic interactions. Importantly, INDUS requires significantly less computational expense than the prior simulation approach, facilitating the comparison of μ_A for a larger range of SAM systems.

We confirmed that SAM order and fluctuations influence interfacial hydrophobicity rather than ligand length itself (*e.g.*, due to varying van der Waals interactions). We simulated a butanethiol SAM at a low temperature (150 K) to increase its order, which we found was similar to that of a dodecanethiol SAM at 300 K (Figure S3). We restrained all heavy atoms of the butanethiol SAM by applying harmonic biases

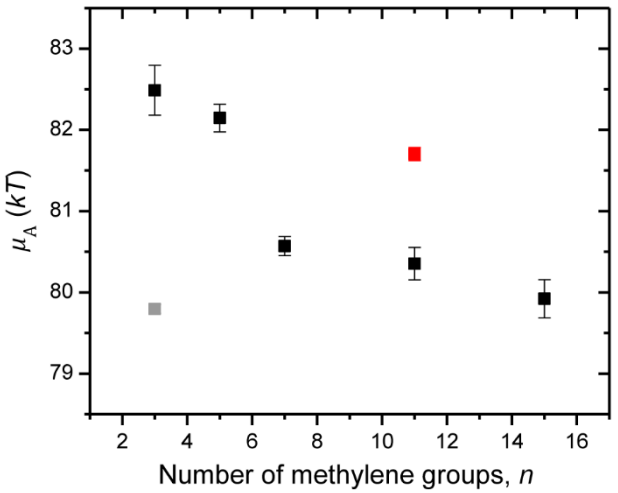

Figure 2. Hydration free energy (μ_A) as a function of the number of methylene groups in the ligand chain. n=3 corresponds to butanethiol and n=11 corresponds to dodecanethiol. The gray square indicates the restrained, ordered butanethiol SAM and the red square indicates the SAM containing unsaturated ligands. Error bars are the standard error from three independent INDUS simulations.

to artificially maintain SAM order and inhibit molecular fluctuations, then performed INDUS at 300 K to measure μ_A. Figure 2 shows that μ_A is similar for both the restrained, ordered butanethiol SAM (indicated by a gray square) and an unrestrained dodecanethiol SAM. This result demonstrates that either SAM order or fluctuations dictate interfacial hydrophobicity independent of ligand length.

We tested the hypothesis that interfacial water molecules relax quickly compared to the timescale for SAM fluctuations by computing autocorrelation times for SAM and water order parameters in unbiased simulations. We calculated three SAM order parameters: (*i*) the hexatic order parameter, ψ_6, which measures the in-plane six-fold symmetry of ligand end group carbon atoms, (*ii*) the tilt angle, θ_{tilt}, which measures the angle formed between the ligand chain and the surface normal, and (*iii*) the root-mean-square deviation, *RMSD*, of ligand heavy atoms relative to their average positions. We also measured the OH orientation angle, θ_{OH}, which measures the angle formed between a water OH bond and the substrate normal. For the n^{th} order parameter, we computed a corresponding autocorrelation time, τ_n, by fitting the autocorrelation function to a stretched exponential, $\exp\left[-(t/\tau_n)^{\beta}\right]$. SAM order parameters were fit with $\beta = 1$ while the OH bond angle was fit with $\beta = 0.5$ based on previous studies of water dynamics within protein hydration shells.[31-33] In addition, we computed the hydrogen bond relaxation time, τ_R, and the average hydrogen bond lifetime, τ_{HB}, per water molecule within 0.5 nm of the SAM surface as other timescales relevant to water relaxation.[34] Additional calculation methods are provided in SI Section S1. Figure 3 compares these six timescales. Order parameters for the butanethiol SAM have shorter autocorrelation times than order parameters for the dodecanethiol SAM, which is consistent with the larger fluctuations of the butanethiol ligands.[23-24] Nonetheless, the timescales for interfacial water relaxation are ~2.5-10 times shorter than those of all SAM order parameters. We conclude that water relaxes quickly compared to SAM fluctuations, suggesting that the order of each SAM configuration sampled due to these fluctuations should dictate hydrophobicity.

To decouple SAM order from molecular fluctuations, we measured μ_A for a series of SAM configurations that were selected to span a range of ψ_6 values to test the hypothesis that ψ_6 and μ_A should be highly correlated if SAM order, and not fluctuations, dictates interfacial hydrophobicity. We selected 60 SAM configurations from simulations of the butanethiol and dodecanethiol SAMs at 300 K and a butanethiol SAM at 200 K (Figure S3) that sampled equally spaced values of ψ_6 between $\psi_6 = 0.19$ (the disordered extreme) to $\psi_6 = 0.78$ (the ordered extreme). Each SAM configuration was restrained as previously described for the restrained, ordered butanethiol SAM and INDUS was performed to compute corresponding values of μ_A. Figure 4A shows that ψ_6 and μ_A are highly correlated (Pearson's r = -0.83; a

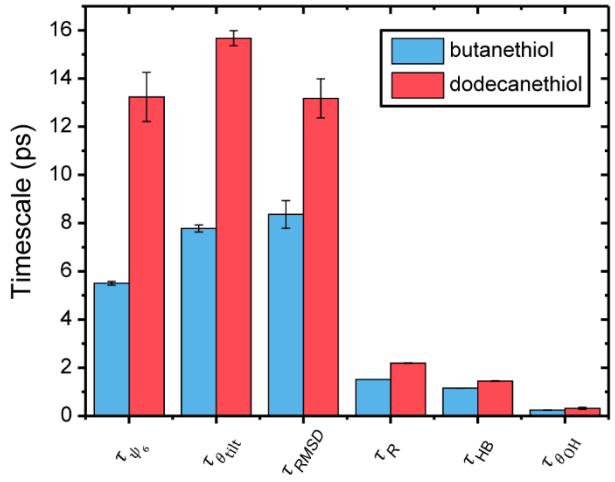

Figure 3. Autocorrelation times for the SAM hexatic order parameter (τ_{ψ_6}), ligand tilt angle ($\tau_{\theta_{\mathrm{tilt}}}$), root-mean-square deviation (τ_{RMSD}), and the OH orientation angle ($\tau_{\theta_{\mathrm{OH}}}$). The hydrogen bonding relaxation time (τ_R) and lifetime (τ_{HB}) are included for comparison. Error bars not seen are smaller than the width of the top line of the column.

value close to -1 indicates total negative linear correlation) with the negative correlation indicating that interfacial hydrophobicity increases with increasing SAM order. Similar trends were found when correlating μ_{A} with two additional SAM order parameters (Figure S8). Figure 4A also shows values of μ_{A} and corresponding ensemble-average values of ψ_6 for the unrestrained butanethiol and dodecanethiol SAMs. These points lie close to the linear fit to the data for restrained SAMs, suggesting that the hydrophobicity of the unrestrained SAMs can also be related primarily to SAM order. The accumulated μ_{A} measurements thus indicate that SAM order primarily dictates interfacial hydrophobicity, while ligand fluctuations cause the SAM to sample configurations of varying order near which interfacial water molecules rapidly relax.

We next sought to determine why the hydrophobicity of SAM configurations varies with order. In the large length scale limit, interfacial hydrophobicity can typically be related to the nonpolar solvent-accessible surface area (SASA),[35-36] which varies because changes to SAM order alter the surface topology. We calculated the SASA using the double cubic lattice method to determine if μ_{A} and SASA are correlated.[37] Figure 4B shows that the SASA and μ_{A} are weakly correlated (Pearson's r = 0.15). The hydrophobicity of a surface is typically assumed to increase with increasing nonpolar SASA[35-36], but Figure 4B shows the opposite behavior: μ_{A} increases, indicating that hydrophobicity decreases, with increasing SASA. This result suggests that SAM order does not influence hydrophobicity by modulating the SASA, but rather by changing interfacial water properties.

To better understand how SAM order impacts hydrophobicity, we related spatial variations in water properties to spatial variations in ligand end group positions. We calculated Voronoi diagrams by projecting the positions of the ligand end group carbon atoms into 2D. A Voronoi diagram shows the bisection of lines connecting the nearest-neighbor points in a plane; the Voronoi diagram for a perfectly ordered SAM would contain perfect hexagons. Water properties were computed within spherical cavities of radius 0.3 nm that were arranged in a grid spanning the SAM surface with cavities spaced by 0.1 nm in both the *x* and *y* dimensions. The center of each cavity was placed 0.3 nm above the SAM surface. In each cavity, we calculated the local hydration free energy, μ_{L}, using Equation 1. μ_{L} differs from μ_{A} by reporting the hydration free energy for a small spherical cavity centered on a specific *x*- and *y*-position rather than for a larger rectangular cavity spanning the SAM surface, thus measuring the hydrophobicity of a small region of the surface. In each cavity, we also computed the average water density, ρ, and the average number of hydrogen bonds per water molecule. All quantities were calculated from 20-ns unbiased simulations as described in SI Section S2.

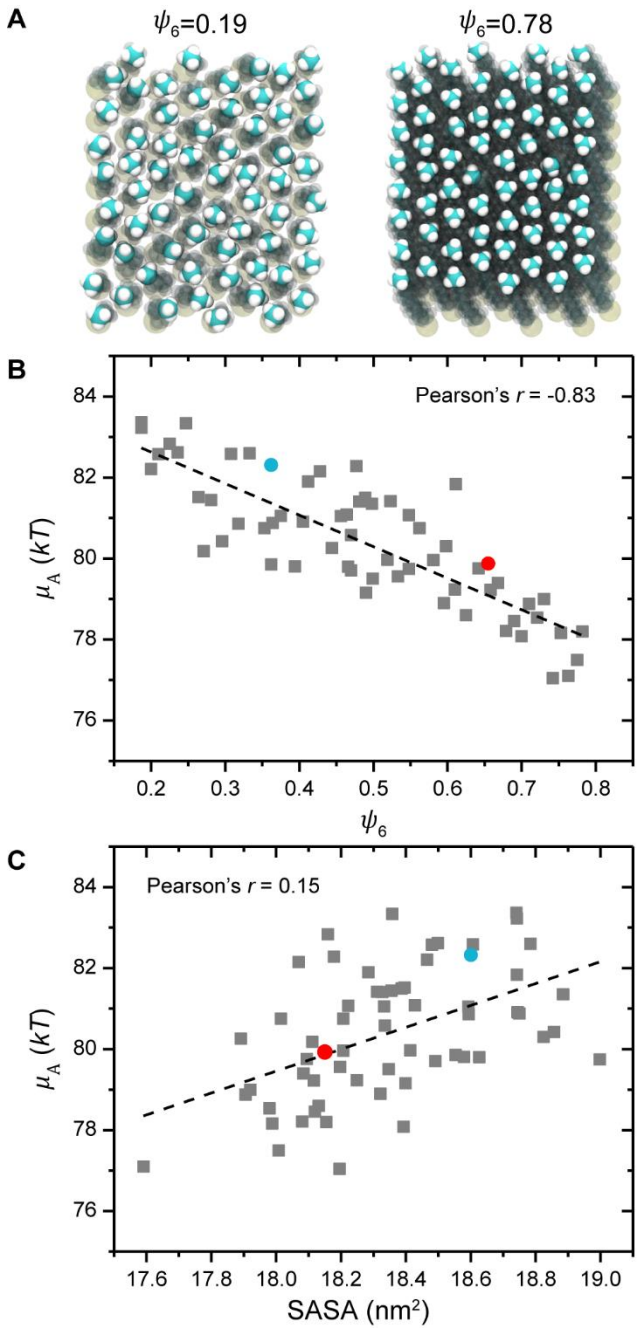

Figure 4. A Top-down simulation snapshots illustrating the disordered (ψ_6=0.19; left) and ordered (ψ_6=0.78) SAMs. Water is not shown for clarity. (**B, C**) Hydration free energy (μ_A) as a function of (**B**) the hexatic order parameter (ψ_6) and (**C**) the solvent accessible-surface area (SASA). Gray squares indicate simulations in which ligand heavy atoms are restrained to inhibit fluctuations and maintain SAM order. The blue circles indicate μ_A computed for the unrestrained butanethiol SAM and corresponding ensemble-average values of either ψ_6 or the SASA. The red circles indicate the same quantities for the unrestrained dodecanethiol SAM.

Figure 5 superimposes the water properties computed in each of the spherical cavities onto the Voronoi diagrams for the restrained SAM configurations at the extremes of the dataset (ψ_6=0.19 and ψ_6=0.78). In general, Figure 5 reveals distinct spatial heterogeneities in the properties of interfacial water molecules near the disordered SAM, whereas the properties of interfacial water molecules near the ordered SAM are more homogeneous. Figure 5A and 5D show that the average water density (normalized by the

bulk water density) is increased along the lines of the Voronoi diagram. These areas are where the free volume between ligands is increased, allowing water molecules to partially embed within the SAM. Figure 5B and 5E show that the areas of increased water density translate to increased values of μ_L, indicating that the embedded water molecules behave like hydrophilic groups at the SAM-water interface to transform the uniformly nonpolar surface into one that appears chemically heterogeneous. Notably, the area over which μ_L increases is larger than the area associated with increased water density. We thus hypothesized that the regions of increased water density could locally pin the SAM-water interface to decrease the hydrophobicity over a larger area due to transverse water-water correlations; prior studies measuring the effects of chemically heterogeneous SAMs on water properties observed similar deformations to the SAM-water interface induced by single and clustered hydroxyl groups on otherwise

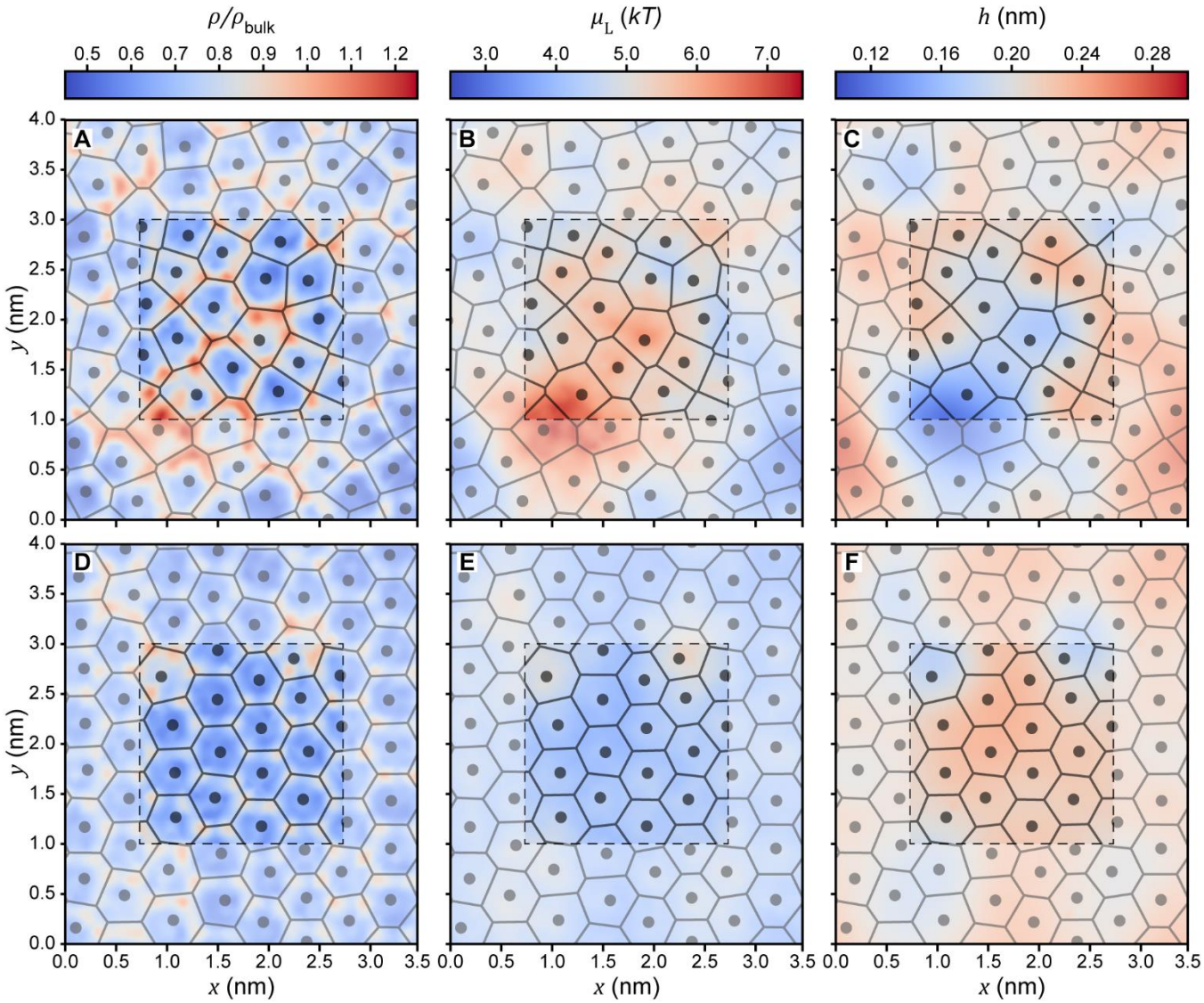

Figure 5. 2D Voronoi diagrams of the ligand end group carbon atoms. **A-C** show diagrams for the disordered (ψ_6=0.19) SAM whereas **D-F** show diagrams for the ordered (ψ_6=0.78) SAM. Black circles indicate the positions of the end group carbon atoms. Superimposed on the Voronoi diagrams are water properties computed in spherical cavities with radii of 0.3 nm. **A** and **D** show normalized water densities (ρ/ρ_{bulk}), **B** and **E** show local hydration free energies (μ_L) , and **C** and **F** show the height of the SAM-water interface above the SAM surface (h). The unshaded region inside the dotted lines indicates the area covered by the cavity biased during INDUS simulations.

nonpolar SAMs.[22, 38] To test this hypothesis, we defined the height of the SAM-water interface, h, as the distance between the isosurface where the average water density is equal to half the bulk water density (*i.e.*, the Willard-Chandler dividing surface[39]) and the SAM surface. Figure 5C and 5F show the spatial dependence in h. As expected, the interface is farther from the SAM surface (larger values of h) for areas corresponding to lower values of μ_{L}, whereas the interface is pinned (smaller values of h) for areas corresponding to larger values of μ_{L} where water molecules embed within the SAM. Figure S9 shows that hydrogen bonding is promoted within these same regions, further confirming an increase in the local water structure that is consistent with our prior work.[24] These findings support the hypothesis that water molecules partially penetrate into the free volume accessible at disordered SAM interfaces to act similarly to hydroxyl functional groups, locally pinning the SAM-water interface and decreasing SAM hydrophobicity.

Our findings indicate that SAM order dictates interfacial hydrophobicity by modulating chemically heterogeneous surface properties which arise due to the penetration of water molecules into the free volume between ligands at disordered SAM interfaces. Ligand fluctuations cause each SAM to sample a range of different configurations with varying order, but otherwise do not significantly affect hydrophobicity because interfacial water molecules quickly relax near each configuration. These findings provide new insight into how spatial variations in water properties cause disordered nonpolar SAMs to appear less hydrophobic than ordered nonpolar SAMs despite seemingly similar chemical properties, building upon our prior study of the average water structure across SAM interfaces.[24] Moreover, this work suggests that disorder could promote spatial heterogeneities and thus modulate interfacial hydrophobicity for rigid surfaces, as has been suggested previously.[25] We expect that variations in interfacial hydrophobicity will be even more pronounced for surfaces with larger variations in free volume, such as SAM-protected nanoparticles with highly curved surfaces.[40] While the values of μ_{A} vary over a small range, prior experimental measurements of hydrophobic interactions between similar SAMs suggest that these changes can lead to a ~4x difference in the magnitude of hydrophobic interactions for macroscopic surfaces.[23-24] Therefore, these findings suggest that tuning the physical properties of a material could be a powerful approach for engineering interfacial hydrophobicity.

Supporting information

Details on simulation preparation, validations, and additional results and discussion.

Author information

The authors declare no competing financial interests.

Acknowledgments

The authors gratefully acknowledge partial support of this research through the University of Wisconsin Materials Research Science and Engineering Center (DMR-1720415). Support for this research was provided by the University of Wisconsin-Madison Office of the Vice Chancellor for Research and Graduate Education with funding from the Wisconsin Alumni Research Foundation. This work used the Extreme Science and Engineering Discovery Environment (XSEDE), which is supported by National Science Foundation grant number ACI-1548562, and the Center for High Throughput Computing at the University of Wisconsin-Madison. The authors also thank Prof. Nicholas L. Abbott and Hongseung Yeon from Cornell University for their insightful discussion.

References

1. Sanchez-Iglesias, A.; Grzelczak, M.; Altantzis, T.; Goris, B.; Perez-Juste, J.; Bals, S.; Van Tendeloo, G.; Donaldson, S. H., Jr.; Chmelka, B. F.; Israelachvili, J. N.; Liz-Marzan, L. M., Hydrophobic interactions modulate self-assembly of nanoparticles. *ACS Nano* **2012,** *6* (12), 11059-65.
2. Van Lehn, R. C.; Alexander-Katz, A., Ligand-mediated short-range attraction drives aggregation of charged monolayer-protected gold nanoparticles. *Langmuir* **2013,** *29* (28), 8788-98.
3. Dill, K. A., Dominant forces in protein folding. *Biochemistry* **1990,** *29* (31), 7133-55.
4. Dobson, C. M., Protein folding and misfolding. *Nature* **2003,** *426* (6968), 884-90.
5. Tanford, C., The hydrophobic effect and the organization of living matter. *Science* **1978,** *200* (4345), 1012-1018.
6. Sprenger, K. G.; Pfaendtner, J., Strong Electrostatic Interactions Lead to Entropically Favorable Binding of Peptides to Charged Surfaces. *Langmuir* **2016,** *32* (22), 5690-701.
7. First, J. T.; Webb, L. J., Agreement between Experimental and Simulated Circular Dichroic Spectra of a Positively Charged Peptide in Aqueous Solution and on Self-Assembled Monolayers. *J Phys Chem B* **2019,** *123* (21), 4512-4526.
8. Ozboyaci, M.; Kokh, D. B.; Corni, S.; Wade, R. C., Modeling and simulation of protein-surface interactions: achievements and challenges. *Q Rev Biophys* **2016,** *49*, e4.
9. Cedervall, T.; Lynch, I.; Lindman, S.; Berggard, T.; Thulin, E.; Nilsson, H.; Dawson, K. A.; Linse, S., Understanding the nanoparticle-protein corona using methods to quantify exchange rates and affinities of proteins for nanoparticles. *Proc Natl Acad Sci U S A* **2007,** *104* (7), 2050-5.
10. Chandler, D., Interfaces and the driving force of hydrophobic assembly. *Nature* **2005,** *437* (7059), 640-7.
11. Patel, A. J.; Varilly, P.; Jamadagni, S. N.; Hagan, M. F.; Chandler, D.; Garde, S., Sitting at the edge: how biomolecules use hydrophobicity to tune their interactions and function. *J Phys Chem B* **2012,** *116* (8), 2498-503.
12. Patel, A. J.; Garde, S., Efficient method to characterize the context-dependent hydrophobicity of proteins. *J Phys Chem B* **2014,** *118* (6), 1564-73.
13. Giovambattista, N.; Lopez, C. F.; Rossky, P. J.; Debenedetti, P. G., Hydrophobicity of protein surfaces: Separating geometry from chemistry. *Proc Natl Acad Sci U S A* **2008,** *105* (7), 2274-9.
14. Stock, P.; Monroe, J. I.; Utzig, T.; Smith, D. J.; Shell, M. S.; Valtiner, M., Unraveling Hydrophobic Interactions at the Molecular Scale Using Force Spectroscopy and Molecular Dynamics Simulations. *ACS Nano* **2017,** *11* (3), 2586-2597.
15. Ma, C. D.; Wang, C.; Acevedo-Velez, C.; Gellman, S. H.; Abbott, N. L., Modulation of hydrophobic interactions by proximally immobilized ions. *Nature* **2015,** *517* (7534), 347-50.
16. Wang, C.; Ma, C. D.; Yeon, H.; Wang, X.; Gellman, S. H.; Abbott, N. L., Nonadditive Interactions Mediated by Water at Chemically Heterogeneous Surfaces: Nonionic Polar Groups and Hydrophobic Interactions. *J Am Chem Soc* **2017,** *139* (51), 18536-18544.
17. Monroe, J. I.; Shell, M. S., Computational discovery of chemically patterned surfaces that effect unique hydration water dynamics. *Proc Natl Acad Sci U S A* **2018**.
18. Schrader, A. M.; Monroe, J. I.; Sheil, R.; Dobbs, H. A.; Keller, T. J.; Li, Y.; Jain, S.; Shell, M. S.; Israelachvili, J. N.; Han, S., Surface chemical heterogeneity modulates silica surface hydration. *Proc Natl Acad Sci U S A* **2018,** *115* (12), 2890-2895.
19. Harris, R. C.; Pettitt, B. M., Effects of geometry and chemistry on hydrophobic solvation. *Proc Natl Acad Sci U S A* **2014,** *111* (41), 14681-6.
20. Jiang, L.; Cao, S.; Cheung, P. P.; Zheng, X.; Leung, C. W. T.; Peng, Q.; Shuai, Z.; Tang, B. Z.; Yao, S.; Huang, X., Real-time monitoring of hydrophobic aggregation reveals a critical role of cooperativity in hydrophobic effect. *Nat Commun* **2017,** *8*, 15639.
21. Wei, W.; Yu, J.; Broomell, C.; Israelachvili, J. N.; Waite, J. H., Hydrophobic enhancement of Dopa-mediated adhesion in a mussel foot protein. *J Am Chem Soc* **2013,** *135* (1), 377-83.

22. Xi, E.; Venkateshwaran, V.; Li, L.; Rego, N.; Patel, A. J.; Garde, S., Hydrophobicity of proteins and nanostructured solutes is governed by topographical and chemical context. *Proc Natl Acad Sci U S A* **2017,** *114* (51), 13345-13350.
23. Yeon, H.; Wang, C.; Van Lehn, R. C.; Abbott, N. L., Influence of Order within Nonpolar Monolayers on Hydrophobic Interactions. *Langmuir* **2017,** *33* (19), 4628-4637.
24. Dallin, B. C.; Yeon, H.; Ostwalt, A. R.; Abbott, N. L.; Van Lehn, R. C., Molecular Order Affects Interfacial Water Structure and Temperature-Dependent Hydrophobic Interactions between Nonpolar Self-Assembled Monolayers. *Langmuir* **2019,** *35* (6), 2078-2088.
25. Shin, S.; Willard, A. P., Water's Interfacial Hydrogen Bonding Structure Reveals the Effective Strength of Surface-Water Interactions. *J Phys Chem B* **2018,** *122* (26), 6781-6789.
26. Porter, M. D.; Bright, T. B.; Allara, D. L.; Chidsey, C. E. D., Spontaneously organized molecular assemblies. 4. Structural characterization of n-alkyl thiol monolayers on gold by optical ellipsometry, infrared spectroscopy, and electrochemistry. *Journal of the American Chemical Society* **1987,** *109* (12), 3559-3568.
27. Love, J. C.; Estroff, L. A.; Kriebel, J. K.; Nuzzo, R. G.; Whitesides, G. M., Self-assembled monolayers of thiolates on metals as a form of nanotechnology. *Chem Rev* **2005,** *105* (4), 1103-69.
28. Patel, A. J.; Varilly, P.; Chandler, D., Fluctuations of water near extended hydrophobic and hydrophilic surfaces. *J Phys Chem B* **2010,** *114* (4), 1632-7.
29. Godawat, R.; Jamadagni, S. N.; Garde, S., Characterizing hydrophobicity of interfaces by using cavity formation, solute binding, and water correlations. *Proc Natl Acad Sci U S A* **2009,** *106* (36), 15119-24.
30. Patel, A. J.; Varilly, P.; Chandler, D.; Garde, S., Quantifying density fluctuations in volumes of all shapes and sizes using indirect umbrella sampling. *J Stat Phys* **2011,** *145* (2), 265-275.
31. Bizzarri, A. R.; Cannistraro, S., Molecular Dynamics of Water at the Protein−Solvent Interface. *The Journal of Physical Chemistry B* **2002,** *106* (26), 6617-6633.
32. Corradini, D.; Strekalova, E. G.; Stanley, H. E.; Gallo, P., Microscopic mechanism of protein cryopreservation in an aqueous solution with trehalose. *Sci Rep* **2013,** *3*, 1218.
33. Fogarty, A. C.; Laage, D., Water dynamics in protein hydration shells: the molecular origins of the dynamical perturbation. *J Phys Chem B* **2014,** *118* (28), 7715-29.
34. Luzar, A.; Chandler, D., Structure and hydrogen bond dynamics of water–dimethyl sulfoxide mixtures by computer simulations. *The Journal of Chemical Physics* **1993,** *98* (10), 8160-8173.
35. Chothia, C., Hydrophobic bonding and accessible surface area in proteins. *Nature* **1974,** *248* (5446), 338-339.
36. Durham, E.; Dorr, B.; Woetzel, N.; Staritzbichler, R.; Meiler, J., Solvent accessible surface area approximations for rapid and accurate protein structure prediction. *J Mol Model* **2009,** *15* (9), 1093-108.
37. Eisenhaber, F.; Lijnzaad, P.; Argos, P.; Sander, C.; Scharf, M., The double cubic lattice method: Efficient approaches to numerical integration of surface area and volume and to dot surface contouring of molecular assemblies. *Journal of Computational Chemistry* **1995,** *16* (3), 273-284.
38. Acharya, H.; Vembanur, S.; Jamadagni, S. N.; Garde, S., Mapping hydrophobicity at the nanoscale: Applications to heterogeneous surfaces and proteins. *Faraday Discussions* **2010,** *146*.
39. Willard, A. P.; Chandler, D., Instantaneous liquid interfaces. *J Phys Chem B* **2010,** *114* (5), 1954-8.
40. Chew, A. K.; Van Lehn, R. C., Effect of Core Morphology on the Structural Asymmetry of Alkanethiol Monolayer-Protected Gold Nanoparticles. *The Journal of Physical Chemistry C* **2018,** *122* (45), 26288-26297.